Since January 2020 Elsevier has created a COVID-19 resource centre with free information in English and Mandarin on the novel coronavirus COVID-19. The COVID-19 resource centre is hosted on Elsevier Connect, the company's public news and information website.

Phytochemistry 135 (2017) 151–159

Contents lists available at ScienceDirect

Phytochemistry

journal homepage: www.elsevier.com/locate/phytochem

Antiproliferative cyclodepsipeptides from the marine actinomycete *Streptomyces* sp. P11-23B downregulating the tumor metabolic enzymes of glycolysis, glutaminolysis, and lipogenesis

Xuewei Ye [a], Komal Anjum [a], Tengfei Song [a], Wenling Wang [a], Ying Liang [a], Mengxuan Chen [a], Haocai Huang [a], Xiao-Yuan Lian [b, **], Zhizhen Zhang [a, *]

[a] Ocean College, Zhoushan Campus, Zhejiang University, Zhoushan 316021, China
[b] College of Pharmaceutical Sciences, Zhejiang University, Hangzhou 310058, China

ARTICLE INFO

Article history:
Received 20 January 2016
Received in revised form
7 December 2016
Accepted 13 December 2016
Available online 31 December 2016

Keywords:
Marine actinomycete
Streptomyces sp.
Cyclodepsipeptides
Antiproliferative agents
Glioma cells
Tumor metabolic regulators

ABSTRACT

Two cyclodepsipeptides and a known cyclodepsipeptide valinomycin were isolated from a culture of the marine actinomycete *Streptomyces* sp. P11-23B. Their structures were established based on NMR, HRESIMS, and MS-MS spectroscopic interpretation as well as by chemical degradation. Both streptodepsipeptides P11A and P11B inhibited proliferation of different glioma cell lines, with IC_{50} values ranging from 0.1 μM to 1.4 μM. Streptodepsipeptide P11A was found to block the cell cycle at the G_0/G_1 phase and induce apoptosis in glioma cells. Further investigation demonstrated that streptodepsipeptide P11A downregulated expression of HK2, PFKFB3, PKM2, GLS, and FASN, important tumor metabolic enzymes. Data from this study suggested that targeting multiple tumor metabolic regulators might be one anti-glioma mechanism of streptodepsipeptide P11A. A possible mechanism for this class of streptodepsipeptides is reported herein.

1. Introduction

Gliomas are the most common and high death malignant brain tumors (Patil et al., 2013; Ru et al., 2013) and can be located at many important brain function areas, which make surgical resection extremely difficult. Therefore, chemotherapy has played a more important role in treatment and prevention of gliomas. However, so far very few drugs have been approved for treating gliomas including temozolomide (TMZ), carmustine, and lomustine. Of these, only TMZ has been independently used for treatment of gliomas. Furthermore, most current anti-glioma drugs are cytotoxicity-based alkylating agents with limited efficacy and serious side-effects (Chamberlain, 2010; Mittal et al., 2015). Therefore, there is an urgent need to discover lead compounds for development of novel anti-glioma drugs. Marine-derived natural products are important sources for discovery of new anticancer drug leads (Newman and Cragg, 2014; Petit and Biard, 2013; Schumacher et al., 2011).

Enhanced glycolysis, elevated glutaminolysis, and exacerbated lipogenesis, which are required for the rapid and unlimited proliferation of tumor cells, have been demonstrated as prominent hallmarks in glioma metabolism (Galluzzi et al., 2013; Guo et al., 2013; Vander Heiden, 2011; Ru et al., 2013). There are several important regulators (enzymes) in the glycolytic pathway, such as hexokinase 2 (HK2) (Vander Heiden, 2011; Wolf et al., 2011), 6-phosphofructo-2-kinase/fructose-2,6-bisphosphatase (PFKFB3) (Kessler et al., 2008; Vander Heiden, 2011), and pyruvate kinase M2 (PKM2) (Kefas et al., 2010; Vander Heiden, 2011), that have been shown to be up-regulated in the glioma cells. These specific regulators are preferentially used by cancer cells (Vander Heiden, 2011). Glutamine metabolism (Daye and Wellen, 2012; Ru et al., 2013) and lipid metabolism (Guo et al., 2013; Ru et al., 2013; Santos and Schulze, 2012) have also been found to be largely altered in cancer cells. Both glutaminase (GLS, a key enzyme of glutaminolysis) (Daye and Wellen, 2012; Lu et al., 2010; Ru et al., 2013) and fatty acid synthase (FASN, a key lipogenic enzyme) (Menendez and Lupu, 2007; Ru et al., 2013) are up-regulated in gliomas. Accumulated

* Corresponding author.
** Corresponding author.
E-mail addresses: xylian@zju.edu.cn (X.-Y. Lian), zzhang88@zju.edu.cn (Z. Zhang).

http://dx.doi.org/10.1016/j.phytochem.2016.12.010
0031-9422/

studies have demonstrated that the above mentioned metabolic enzymes are promising targets for discovery of novel anticancer drugs.

As part of an ongoing project for discovery of novel anti-glioma and antibacterial compounds from marine resources (Chen et al., 2015; Liang et al., 2016; Xin et al., 2012; Yu et al., 2014, 2015), a crude extract prepared from the culture of marine bacterium strain P11-23B was found to significantly inhibit proliferation of human glioma cells. Chemical investigation of this active extract led to isolation of two new cyclodepsipeptides, which were named as streptodepsipeptides P11A (**2**) and P11B (**3**), together with known valinomycin (**1**) (Fig. 1). This study described the isolation and culture of the strain P11-23B, the isolation and structural elucidation of new compounds, and their bioactivity against glioma cells and effect on the tumor metabolic regulators.

2. Results and discussion

Strain P11-23B was isolated from a marine mud sample and assigned as *Streptomyces* sp. P11-23B based on the analysis of its 16S rDNA gene sequence, which matched (99% identity for a 1361 bp stretch of sequence) those of seven *Streptomyces* strains (Supplementary Data, Figure S_1 and Table S_1). Culture of this marine actinomycete was grown in Gause's liquid medium (50.0 L). The extract prepared from the culture of P11-23B showed significant activity against the proliferation of human glioma cells with inhibitions of 87.17% for glioma U87-MG cells and 86.84% for U251 cells. Separation of this active extract by ODS column chromatography, following by HPLC purification, afforded three compounds **1**–**3**.

Compound **1** was proved to be the known cyclodepsipeptide valinomycin based on its NMR and HRESIMS data, melting point, optical rotation value, the analysis of its acidic hydrolysates by chiral HPLC and GC analyses, and the comparison with literature data (Pettit et al., 1999; Tabeta and Saito, 1985). Valinomycin (**1**) was previously isolated from several *Streptomyces* species (Heisey et al., 1988; Lim et al., 2007; Park et al., 2008; Pettit et al., 1999) and is well known to enhance the K^+ permeability of several membrane systems including mitochondria, erythrocytes, and lipid bilayers (Bhattacharyya et al., 1971; Haynes et al., 1969). This cyclodepsipeptide was also reported to have activities against tumors, bacteria, fungi (Lim et al., 2007; Park et al., 2008; Pettit et al., 1999), and severe acute respiratory-syndrome coronavirus (Wu et al., 2004). Valinomycin (**1**) is composed of four units of D-valine (D-Val), L-valine (L-Val), D-α-hydroxyisovaleric acid (D-Hiv), and L-lactate (L-Lac) with a trimer structure of cyclo-(D-Val-L-Lac-L-Val-D-Hiv)$_3$. For its ^{13}C and ^1H NMR spectroscopic data assignments, see Table S_2 (Supplementary Data). It was noted that each of the four units displayed characteristic NMR signals, which allowed for differentiation of the four units. The unit L-Lac was easily recognized by its NMR signals of δ_C 172.7 (C-1), 70.4 (C-2), 17.3 (C-3) and δ_H 5.32 (1H, q, J = 7.0 Hz, H-2) and 1.44 (3H, d, J = 7.0 Hz, H-3), while D-Hiv had its characteristic signals of δ_C 171.0 (C-1), 78.7 (C-2), 30.4 (C-3), 16.8 (C-4) and δ_H 5.02 (1H, d, J = 3.11 Hz, H-2). The D-Val and L-Val could be distinguished from their chemical shifts of C-1, C-2, H-2 and the coupling constant values of $^3J_{CH\text{-}NH}$. The unit D-Val was indicated by its characteristic NMR signals at δ_C 170.2 (C-1), 59.1 (C-2) and δ_H 4.10 (1H, dd, J = 10.0, 8.1 Hz, H-2), 7.88 (1H, d, J = 8.1 Hz, NH-2), as compared with their counterparts of L-Val at δ_C 172.0 (C-1), 60.6 (C-2) and δ_H 3.96 (1H, dd, J = 10.2, 6.2 Hz, H-2), 7.80 (1H, d, J = 6.2 Hz, NH-2). All of these characteristic NMR signals mentioned above are very helpful for the structure elucidation of the new compounds of streptodepsipeptides P11A (**2**) and P11B (**3**), which had very complicated NMR signals.

The HRESIMS spectrum of compound **2** displayed ions at m/z 1095.6051 ($[M-H]^-$) and 1097.6227 ($[M+H]^+$), corresponding to the molecular formula of $C_{53}H_{88}N_6O_{18}$. Its ^{13}C NMR spectrum showed 53 carbon resonances, which were distributed in six zones. The first zone displayed 12 carbonyl carbon (C=O) signals at δ_C 170.28–172.80. Six carbon signals at δ_C 70.41–78.93 in the second zone were assigned to six oxymethines (α–CH–O) and six resonances at δ_C 58.98–60.75 in the third zone were contributed to six nitrogenated methines (α–CH–N). The fourth zone exhibited eight methines (β-CH) at δ_C 28.49–30.41 and one carbon signal at δ_C 25.16 in the fifth zone was assigned to a methylene (β-CH_2). The remaining 20 carbons, which appeared at δ_C 9.41–19.92 in the sixth zone, were assigned to 20 methyls (γ-CH_3 or β-CH_3). The ^1H NMR spectrum of **2** also showed six NH signals at δ_H 7.89 (d, 7.9 Hz), 7.84 (d, 6.0 Hz), 7.83 (d, 8.0 Hz), 7.83 (d, 8.0 Hz), 7.77 (d, 6.2 Hz), and 7.76 (d, 5.8 Hz). All of the above data suggested that compound **2** was composed of 12 units, including six amide groups (amino acids) and six ester groups. Acid hydrolysis of **2** produced D-Val, L-Val, D-Hiv, L-Lac, D-2-hydroxybutanoic acid (D-Hba) as determined by chiral HPLC and GC analyses using the standard compounds as references. Detailed COSY, HSQC, and HMBC spectroscopic analyses confirmed the presence of 12 units including three L-lactates, three L-valines, three D-valines, two D-α-hydroxyisovaleric acids, and one D-2-hydroxybutanoic acid (D-Hba). As shown in Fig. 2, the α-NH and α-CH protons of each valine had a COSY correlation, while the α-CH proton of each unit displayed a COSY correlation with the β-CH (or β-CH_2 for D-Hba, or β-CH_3 for L-Lac) proton, which was correlated with the γ-CH_3 proton. HMBC correlations (see Table 1 and Fig. 2) further supported the structure of each unit. According to the foregoing NMR correlations and the NMR data comparison of

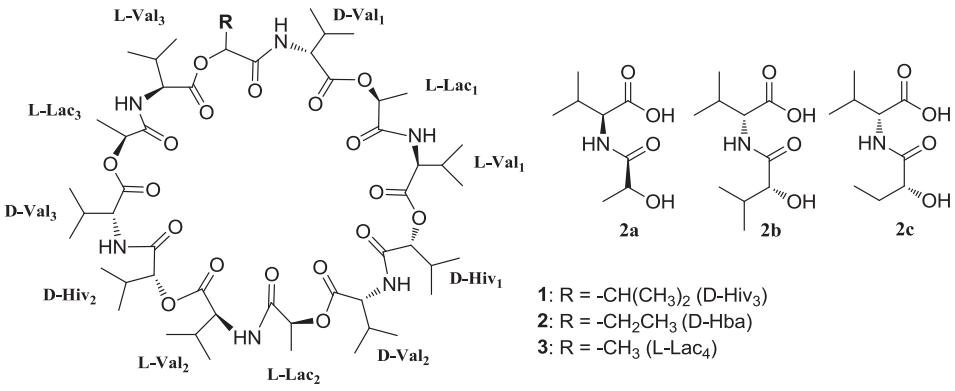

Fig. 1. Structures of compounds **1**–**3**, **2a**, **2b**, and **2c**.

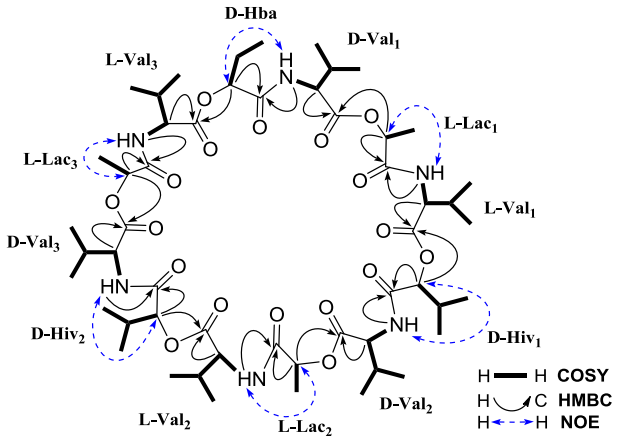

Fig. 2. COSY, key HMBC and NOE correlations of streptodepsipeptide P11A (**2**).

compounds **2** and **1**, it was concluded that the D-Hba unit had its characteristic NMR signals at δ_C 171.40 (C-1), 75.56 (C-2), 25.16 (C-3), 9.41 (C-4) and δ_C 5.11 (1H, dd, J = 6.6, 4.3 Hz, H-2), three L-Lac units resonated at δ_C 172.80, 172.65, 172.55 (C-1), 70.61, 70.53, 70.41 (C-2), 17.44, 17.37, 17.23 (C-3) and δ_H 5.33, 5.33, 5.27 (each 1H, q, J = 6.8 Hz, H-2), and two D-Hiv units displayed at δ_C 171.16, 170.86 (C-1), 78.93, 78.69 (C-2), 30.41, 30.41 (C-3), 16.84, 16.80 (C-4) and δ_H 4.99, 5.02 (each 1H, d, J = 3.2 Hz, H-2). Similarly, the C-1 and C-2 of L-Val and D-Val exhibited different ^{13}C chemical shifts, which were observed at δ_C 171.50–172.22 (>δ 171.0, C-1) and δ_C 60.11–60.75 (>δ 60.0, C-2) for L-Val, and δ_C 170.28–170.42 (<171.0, C-1) and δ_C 58.98–59.25 (<60.0, C-2) for D-Val. The coupling constant values of $^3J_{CH\text{-}NH}$ for the two valines were also different with 5.8–6.2 Hz for L-Val and 7.9–8.0 Hz for D-Val.

The sequence of the 12 units of compound **2** was established based on the following HMBC and NOESY correlations (Table 1 and Fig. 2): HMBC correlations of D-Val$_1$-NH-2 (δ 7.83, d, 8.0 Hz) with D-Hba-C-1 (δ 171.40), L-Lac$_1$-H-2 (δ 5.33) with D-Val$_1$-C-1 (δ 170.28), L-Val$_1$-NH-2 (δ 7.76, d, 5.8 Hz) with L-Lac$_1$-C-1 (δ 172.65), D-Hiv$_1$-H-2 (δ 4.99) with L-Val$_1$-C-1 (δ 172.22), D-Val$_2$-NH-2 (δ 7.83, d, 8.0 Hz) with D-Hiv$_1$-C-1 (δ 170.86), L-Lac$_2$-H-2 (δ 5.27) with D-Val$_2$-C-1 (δ 170.42), L-Val$_2$-NH-2 (δ 7.84, d, 6.0 Hz) with L-Lac$_2$-C-1 (δ 172.80), D-Hiv$_2$-H-2 (δ 5.02) with L-Val$_2$-C-1 (δ 172.06), D-Val$_3$-NH-2 (δ 7.89, d, 7.9 Hz) with D-Hiv$_2$-C-1 (δ 171.16), L-Lac$_3$-H-2 (δ 5.33) with D-Val$_3$-C-1 (δ 170.39), L-Val$_3$-NH-2 (δ 7.77, d, 6.2 Hz) with L-Lac$_3$-C-1 (δ 172.55), D-Hba-H-2 (δ 5.11) with L-Val$_3$-C-1 (δ 171.50); and NOE correlations of D-Val$_1$-NH-2 (δ 7.83) with D-Hba-H-2 (δ 5.11), L-Val$_1$-NH-2 (δ 7.76) with L-Lac$_1$-H-2 (δ 5.33), D-Val$_2$-NH-2 (δ 7.83) with D-Hiv$_1$-H-2 (δ 4.99), L-Val$_2$-NH-2 (δ 7.84) with L-Lac$_2$-H-2 (δ 5.27), D-Val$_3$-NH-2 (δ 7.89) with D-Hiv$_2$-H-2 (δ 5.02), L-Val$_3$-NH-2 (δ 7.77) with L-Lac$_3$-H-2 (δ 5.33).

In order to further confirm the locations of L-Val and D-Val, compound **2** was partially hydrolyzed using 3N LiOH to produce three dipeptides of L-Lac-L-Val (**2a**), D-Hiv-D-Val (**2b**), and D-Hba-D-Val (**2c**). The structures (Fig. 1) of **2a**, **2b**, and **2c** were deduced from their HRESIMS and ^1H NMR data. Further acid hydrolysis of **2a**, **2b**, and **2c** furnished free amino acids of L-Val for **2a** and D-Val for **2b** and **2c**, which were confirmed by chiral HPLC analysis using the standard amino acids as references.

The sequence of the 12 units of compound **2** was also supported from the results of MS-MS analysis. In the MS-MS spectrum

Table 1
^{13}C (125 MHz) and ^1H (500 MHz) NMR spectroscopic data of streptodepsipeptide P11A (**2**, in $CDCl_3$).

	δ_C, type	δ_H (J in Hz)	HMBC (H to C)		δ_C, type	δ_H (J in Hz)	HMBC (H to C)
C=O				Val	28.77, CH	2.35, m	C_1, C_2, C_4, C_5
L-Lac$_1$	172.65, C				28.61, CH	2.32, m	C_1, C_2, C_4, C_5
L-Lac$_2$	172.80, C				28.67, CH	2.33, m	C_1, C_2, C_4, C_5
L-Lac$_3$	172.55, C				28.59, CH	2.27, m	C_1, C_2, C_4, C_5
L-Val$_1$	172.22, C				28.59, CH	2.23, m	C_1, C_2, C_4, C_5
L-Val$_2$	172.06, C				28.49, CH	2.25, m	C_1, C_2, C_4, C_5
L-Val$_3$	171.50[a], C			D-Hiv	30.41, CH	2.37, m	C_1, C_2, C_4, C_5
D-Hiv$_1$	170.86, C				30.41, CH	2.37, m	C_1, C_2, C_4, C_5
D-Hiv$_2$	171.16, C			**γ–CH$_3$**			
D-Hba	171.40[a] C			Val, D-Hiv	19.92, CH_3	0.95–1.10	C_2, C_3
D-Val$_1$	170.28[b], C				19.87, CH_3	0.95–1.10	C_2, C_3
D-Val$_2$	170.42[b]C				19.70, CH_3	0.95–1.10	C_2, C_3
D-Val$_3$	170.39[b], C				19.70, CH_3	0.95–1.10	C_2, C_3
α–CH–O					19.67, CH_3	0.95–1.10	C_2, C_3
D-HiV$_1$	78.93, CH	4.99, d (3.2)	C_1, C_3, C_4, C_5, L-Val$_1$-C_1		19.64, CH_3	0.95–1.10	C_2, C_3
D-HiV$_2$	78.69, CH	5.02, d (3.2)	C_1, C_3, C_4, C_5, L-Val$_2$-C_1		19.64, CH_3	0.95–1.10	C_2, C_3
D-Hba	75.56, CH	5.11, dd (6.6, 4.3)	C_1, C_3, C_4, L-Val$_3$-C_1		19.60, CH_3	0.95–1.10	C_2, C_3
L-Lac$_1$	70.41[c], CH	5.33, q (6.8)	C_1, C_3, D-Val$_1$-C_1		19.58, CH_3	0.95–1.10	C_2, C_3
L-Lac$_2$	70.61[c], CH	5.27, q (6.8)	C_1, C_3, D-Val$_2$-C_1		19.38, CH_3	0.95–1.10	C_2, C_3
L-Lac$_3$	70.53[c], CH	5.33, q (6.8)	C_1, C_3, D-Val$_3$-C_1		19.38, CH_3	0.95–1.10	C_2, C_3
α–CH–N					19.36, CH_3	0.95–1.10	C_2, C_3
L-Val$_1$	60.75, CH	3.96, dd (10.0, 5.8)	C_1, C_3, C_4, C_5		19.26, CH_3	0.95–1.10	C_2, C_3
L-Val$_2$	60.68, CH	3.97, dd (10.0, 6.0)	C_1, C_3, C_4, C_5		19.26, CH_3	0.95–1.10	C_2, C_3
L-Val$_3$	60.11, CH	4.01, dd (10.0, 6.2)	C_1, C_3, C_4, C_5	D-Hiv	16.84, CH_3	0.98	C_2, C_3
D-Val$_1$	58.98, CH	4.13, dd (9.8, 8.0)	C_1, C_3, C_4, C_5		16.80, CH_3	0.98	C_2, C_3
D-Val$_2$	59.25, CH	4.08, dd (9.2, 8.0)	C_1, C_3, C_4, C_5	D-Hba	9.41, CH_3	0.95	C_2, C_3
D-Val$_3$	59.25, CH	4.08, dd (9.2, 7.9)	C_1, C_3, C_4, C_5	**NH**			
β–CH$_3$				L-Val$_1$		7.76, d (5.8)	C_2, C_3, L-Lac$_1$-C_1
L-Lac	17.44, CH_3	1.44–1.47	C_1, C_2	L-Val$_2$		7.84, d (6.0)	C_2, C_3, L-Lac$_2$-C_1
	17.37, CH_3	1.44–1.47	C_1, C_2	L-Val$_3$		7.77, d (6.2)	C_2, C_3, L-Lac$_3$-C_1
	17.23, CH_3	1.44–1.47	C_1, C_2	D-Val$_1$		7.83, d (8.0)	C_2, C_3, D-Hba-C_1
β–CH$_2$				D-Val$_2$		7.83, d (8.0)	C_2, C_3, D-Hiv$_1$-C_1
D-Hba	25.16, CH_2	1.91, m	C_1, C_2, C_4,	D-Val$_3$		7.89, d (7.9)	C_2, C_3, D-Hiv$_2$-C_1
β–CH							

[a-c] The data with the same labels in each column may be interchanged.

(Fig. S_{51}, Supplementary Data), compound **2** displayed a series of ion peaks at *m/z* 1051.6179 (calcd for $C_{52}H_{87}N_6O_{16}^+$, 1051.6173), 870.5064 (calcd for $C_{42}H_{72}N_5O_{14}^+$, 870.5070), 699.4159 (calcd for $C_{34}H_{59}N_4O_{11}^+$, 699.4175), 514.3119 (calcd for $C_{25}H_{44}N_3O_8^+$, 514.3123), 343.2227 (calcd for $C_{17}H_{31}N_2O_5^+$, 343.2227), 200.1282 (calcd for $C_{10}H_{18}NO_3^+$, 200.1281), which were from fragmentations after ring-opening at the ester position with loss of formic acid (CH_2O_2) (Fig. S_{52}), and a series of ion peaks at *m/z* 1069.6273 (calcd for $C_{52}H_{89}N_6O_{17}^+$, 1069.6279), 898.5340 (calcd for $C_{44}H_{76}N_5O_{14}^+$, 898.5383), 699.4159 (calcd for $C_{34}H_{59}N_4O_{11}^+$, 699.4175), 528.3224 (calcd for $C_{26}H_{46}N_3O_8^+$, 528.3279), 329.2076 (calcd for $C_{16}H_{29}N_2O_5^+$, 329.2071), 144.1027 (calcd for $C_7H_{14}NO_2^+$, 144.1019), which were from fragmentations after ring-opening at the amide position with loss of carbon monoxide (CO) (Fig. S_{53}). Both compounds **1** and **2** were isolated from strain P11-23B and might have the same overall biosynthetic pathway, suggesting **1** and **2** should have a similar sequence for the 12 units. Based on the above evidence, the structure of **2** was determined as cyclo-(D-Val-L-Lac-L-Val-D-Hiv-D-Val-L-Lac-L-Val-D-Hiv-D-Val-L- Lac-L-Val-D-Hba), a new cyclodepsipeptide, named as streptodepsipeptide P11A. Its ^{13}C and ^1H NMR data are listed in Table 1.

The molecular formula of $C_{52}H_{86}N_6O_{18}$ for compound **3** was deduced from its $[M-H]^-$ HRESIMS ion at *m/z* 1081.5899 (calcd for $C_{52}H_{85}N_6O_{18}$, 1081.5920), 14 mass units lower than that of **2**. Its ^{13}C NMR spectrum showed 52 carbon signals for 12 carbonyls (δ_C 170.20–172.98), six oxymethines (δ_C 70.33–79.21), six nitrogenated methines (δ_C 58.75–60.97), eight methines (δ_C 28.46–30.43), and 20 methyls (δ_C 16.78–20.03). Acid hydrolysates of **3** were found to be D-Val, L-Val, D-Hiv, and L-Lac as determined by chiral HPLC and GC. Further detailed NMR spectroscopic analysis, in combination with the HRESIMS data, indicated that the structure of **3** was very similar to that of **2**, except for another L-Lac moiety in **3** instead of the D-Hba moiety in **2**. The ^{13}C and ^1H NMR data (Table 2) of **3** were assigned based on the HSQC and HMBC correlations and by comparison of its NMR data with those of compounds **2** and **1**. The structure of **3** was thus elucidated as cyclo-(D-Val-L-Lac-L-Val-D- Hiv-D-Val-L-Lac-L-Val-D-Hiv-D-Val-L-Lac-L-Val-L-Lac), named as streptodepsipeptide P11B, a new cyclodepsipeptide.

Three isolated cyclodepsipeptides (**1**–**3**) were assayed for their activity against the proliferation of four different glioma cell lines by SRB method. The results (Fig. 3 and Table 3) showed that new streptodepsipeptides P11A (**2**) and P11B (**3**) had potent activity with IC_{50} values of 0.3–0.4 μM for **2** and 0.1–1.4 μM for **3**, while known valinomycin (**1**) showed much stronger antiproliferative activity with IC_{50} values ranging from 7.6 to 30.0 nM, probably because of its symmetrical trimer structure (Pettit et al., 1999). The control doxorubicin (DOX) had activity with IC_{50} 0.4–3.3 μM. The two new compounds were also tested for activity in inhibiting growth of normal human astrocytes (HA). As shown in Table 3, the ratios of IC_{50} for HA to glioma cells were within the ranges of 23–30 for **2** and 3–35 and for **3**.

Streptodepsipeptide P11A (**2**) was also assayed for its ability to arrest the cell cycle and induce apoptosis in glioma cells. Flow cytometric analysis was used to measure the DNA content to determine if an alteration of the cell cycle occurred following the treatment of streptodepsipeptide P11A (**2**). U87-MG cells were incubated with 0.8 μM streptodepsipeptide P11A (**2**), DOX (0.8 μM) as positive control, or without compound treatment as negative control (CON) for 12 h and then stained with PI and subjected to flow cytometric analysis. The percentages of each phase in the cell cycle were described in Fig. 4 and Table 4. Cell population at the G_0/G_1 phase was significantly increased by 40.92% after the treatment of 12 h, when compared to the control (CON). This alteration indicated that streptodepsipeptide P11A (**2**) blocked U87-MG cell cycle at the G_0/G_1 phase. Positive control DOX (0.8 μM) also had a 49.69% increasement of DNA content at the G_0/G_1 phase. A similar result was also obtained from the streptodepsipeptide P11A-treated U251 cells (Fig. 4 and Table 4). Flow cytometric analysis with annexin V-FITC/PI double staining was applied to quantify the apoptosis induced by streptodepsipeptide P11A (**2**). After 72 h of treatment, streptodepsipeptide P11A (**2**) (0.8 μM) caused an increase of 20.40% in total apoptotic cells (early and late apoptotic cells), when compared to the control (CON, Fig. 5).

Streptodepsipeptide P11A (**2**) was further investigated for its effects on several important tumor metabolic regulators including HK2 (glycolysis), PFKFB3 (glycolysis), PKM2 (glycolysis), GLS (glutaminolysis), and FASN (lipogenesis). Firstly, the expression levels

Table 2
^{13}C (125 MHz) and ^1H (500 MHz) NMR spectroscopic data of streptodepsipeptide P11B (**3**, in $CDCl_3$).

	δ_C, type	δ_H (*J* in Hz)		δ_C, type	δ_H (*J* in Hz)		δ_C, type	δ_H (*J* in Hz)
C=O			D-Val_1	59.62, CH	4.05, dd (10.0, 7.6)		19.58, CH_3	0.95–1.10
	172.98, C			59.33, CH	4.07, dd (10.0, 8.2)		19.53, CH_3	0.95–1.10
	172.52, C			58.75, CH	4.16, dd (9.8, 8.2)		19.50, CH_3	0.95–1.10
	172.44, C		**β–CH$_3$**				19.47, CH_3	0.95–1.10
	172.34, C		L-Lac	17.73, CH_3	1.44–1.49		19.44, CH_3	0.95–1.10
	172.28, C			17.69, CH_3	1.44–1.49		19.40, CH_3	0.95–1.10
	172.07, C			17.54, CH_3	1.44–1.49		19.33, CH_3	0.95–1.10
	171.49, C			17.11, CH_3	1.44–1.49		19.22, CH_3	0.95–1.10
	170.85, C		**β–CH**			D-Hiv	16.91, CH_3	0.98
	170.72, C		D-Hiv	30.43, CH	2.36, m		16.78, CH_3	0.98
	170.64 C			30.43, CH	2.36, m	**NH**		
	170.49, C		Val	28.92, CH	2.17–2.40	L-Val		7.74, d (5.9)
	170.20, C			28.71, CH	2.17–2.40			7.78, d (6.3)
α–CH–O				28.68, CH	2.17–2.40			7.96, d (6.0)
D-Hiv	79.21, CH	4.94, d (3.2)		28.68, CH	2.17–2.40	D-Val		7.79, d (8.2)
	78.57, CH	5.04, d (3.0)		28.59, CH	2.17–2.40			7.79, d (8.2)
L-Lac	71.20, CH	5.22, q (7.0)		28.46, CH	2.17–2.40			8.00, d (7.6)
	71.00, CH	5.20, q (7.0)	**γ–CH$_3$**					
	70.75, CH	5.32, q (7.0)	Val, D-Hiv	20.03, CH_3	0.95–1.10			
	70.33, CH	5.31, q (7.0)		19.87, CH_3	0.95–1.10			
α–CH–N				19.76, CH_3	0.95–1.10			
L-Val	60.97, CH	3.91, dd (10.0, 5.9)		19.76, CH_3	0.95–1.10			
	60.71, CH	3.96, dd (10.0, 6.3)		19.65, CH_3	0.95–1.10			
	59.78, CH	4.01, dd (9.8, 6.0)		19.63, CH_3	0.95–1.10			

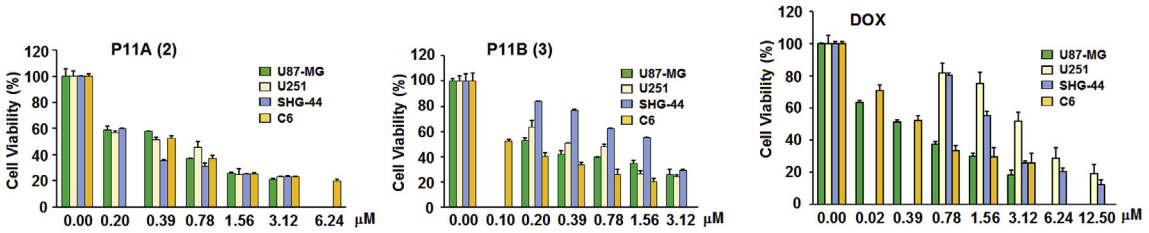

Fig. 3. Streptodepsipeptides P11A (**2**) and P11B (**3**) inhibited the proliferation of glioma cells. Glioma cells were treated with streptodepsipeptides P11A (**2**) and P11B (**3**) or DOX as drug positive control or without compound as negative control for 72 h at different concentrations. Values are means ± S.D. from five independent experiments.

Table 3
Activity of streptodepsipeptides P11A (**2**) and P11B (**3**) inhibiting proliferation of glioma cells (IC_{50}: μM).

Compounds	Glioma Cells (GC)				human astrocytes (HA)
	U251	U87-MG	SHG-44	C6	
Valinomycin (**1**)	7.6 ± 0.7[a]	30.0 ± 2.8[a]	21.0 ± 2.9[a]	24.0 ± 2.0[a]	NT
P11A (**2**)	0.4 ± 0.0	0.4 ± 0.0	0.3 ± 0.0	0.3 ± 0.0	9.1 ± 0.2
Ratios of IC_{50HA}/IC_{50GC}	23	23	30	30	
P11B (**3**)	0.5 ± 0.0	0.2 ± 0.0	1.4 ± 0.2	0.1 ± 0.0	3.5 ± 0.5
Ratios of IC_{50HA}/IC_{50GC}	7	18	3	35	
Doxorubicin (DOX)	3.3 ± 0.7	0.4 ± 0.0	1.9 ± 0.0	0.5 ± 0.1	8.7 ± 1.2
Ratios of IC_{50HA}/IC_{50GC}	3	22	5	17	

[a] The unit of the IC_{50} values is nM, NT: No testing.

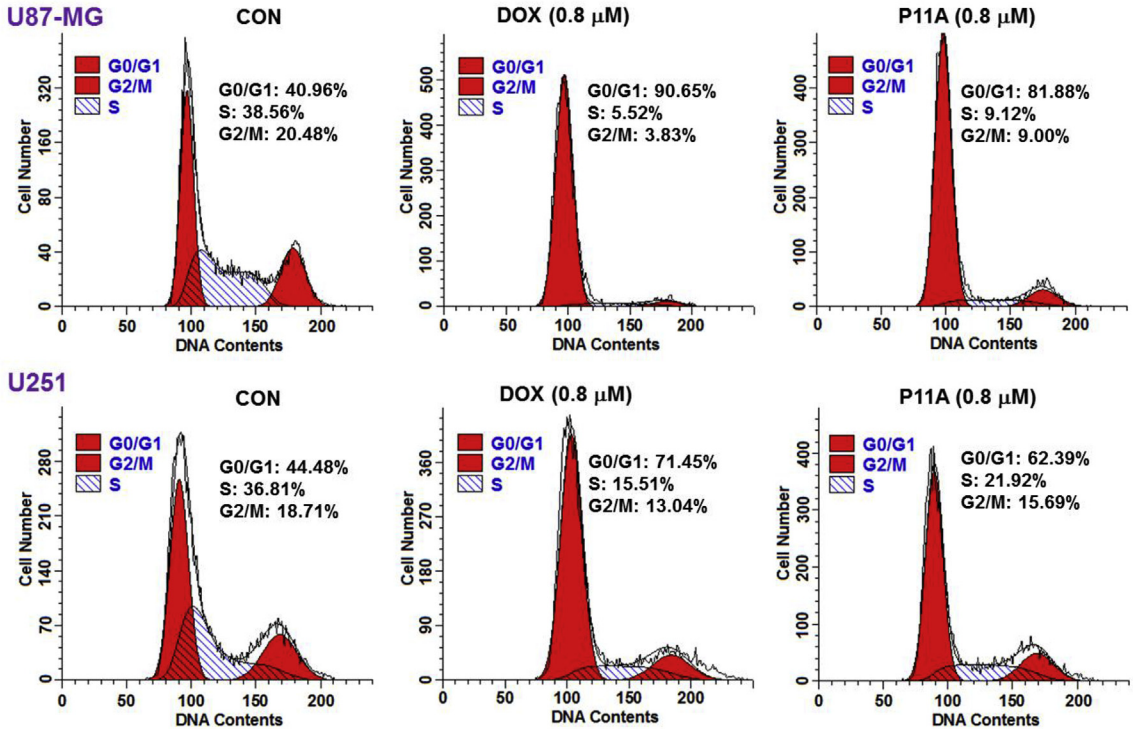

Fig. 4. Streptodepsipeptide P11A (**2**) arrested cell cycle in U87-MG and U251 cells. U87-MG and U251 cells were incubated with streptodepsipeptide P11A (**2**) (0.8 μM), DOX (0.8 μM) as positive control, or without compound treatment as negative control (CON) for 12 h and then stained with PI and subjected to flow cytometric analysis for cell distribution at each phase of cell cycle. Percentage of cells at each stage of the cell cycle was shown. The proportion of cells in the G_0/G_1 phase of the cell cycle was greatly enhanced.

of HK2, PFKFB3, PKM2, GLS, and FASN in four different glioma cell lines of SHG-44, U87-MG, U251, and C6 were tested by western blot. It has been found that all five tumor metabolic regulators were highly expressed in the U87-MG cells (Fig. 6A). Thus, the effects of streptodepsipeptide P11A (**2**) on expression levels of these regulators in the U87-MG cells were evaluated. U87-MG cells were treated by streptodepsipeptide P11A (**2**) (5 μM or 10 μM) for 48 h. Protein prepared from the streptodepsipeptide P11A-treated U87-MG cells was subjected to western blot analysis. The results (Fig. 6B) indicated that HK2, PFKFB3, GLS, and FASN were highly down-regulated in the streptodepsipeptide P11A-treated U87-MG cells, when compared to negative control (CON, U87-MG cells

Table 4
Analysis of cell cycle in streptodepsipeptide P11A-treated U87-MG and U251 cells.

Treatment (12 h)	G_0/G_1	S	G_2/G_M	$Compound_{(G0/G1)}-CON_{(G0/G1)}$
U87-MG				
Control (CON) [a]	40.96%	38.56	20.48	
DOX (0.8 μM)	90.65%	5.52%	3.83%	49.69%
P11A (**2**, 0.8 μM)	81.88%	9.12%	9.00%	40.92%
U251				
Control (CON) [a]	44.48%	36.81%	18.71%	
DOX (0.8 μM)	71.45%	15.51%	13.04%	26.97%
P11A (**2**, 0.8 μM)	62.39%	21.92%	15.69%	17.91%

[a] Control (CON): U87-MG and U251 cells were treated without compounds.

without streptodepsipeptide P11A treatment), while PKM2 was slightly down-regulated. Similar results were also obtained for the known valinomycin (**1**). As shown in Fig. S_{83}, valinomycin (**1**) remarkably reduced expression levels of HK2, FANS, GLS, and had little effect on the downregulation of PKM2. In order to determine if streptodepsipeptide P11A (**2**) selectively affected the expressions of these tumor metabolic enzymes, its effects on regulation of aconitase 2 (ACO2), ATP synthase beta (ATPB), and cytochrome C (Cyto-C) were also investigated [ACO2, ATPB, and Cyto-C are important regulators in the processes of tricarboxylic acid cycle and oxidative phosphorylation, which are the predominant metabolic processes of glucose in the normal cells (Galluzzi et al., 2013; Jones and Schulze, 2012)]. As presented in Fig. 6C, streptodepsipeptide P11A (**2**) had no obvious effects on ACO2 and ATPB expression levels, but increased the level of Cyto-C. These data suggested that streptodepsipeptide P11A (**2**) might selectively regulate tumor metabolic regulators of HK2, PFKFB3, PKM2, GLS, and FASN. The increased expression level of Cyto-C also implied that streptodepsipeptide P11A (**2**) might change the tumor metabolic pathway to the process of oxidative phosphorylation.

Valinomycin (**1**) is known to induce uptake of potassium in membrane of erythrocyte (Bhattacharyya et al., 1971). Therefore, the ability of streptodepsipeptide P11A (**2**) to enhance the K^+ permeability of human erythrocytes was also evaluated. Human erythrocytes were treated with tested compound (**2**) or positive control valinomycin (**1**) for 90 min. The results (Table 5) showed that streptodepsipeptide P11A (**2**) at concentrations of 0.01 μM, 0.05 μM, and 0.1 μM induced 22.36%, 66.46%, and 86.10% increase of intracellular K^+ in erythrocytes, respectively, when compared to the negative control (CON, human erythrocyte without compound treatment). The positive control valinomycin (**1**) at the same concentrations also enhanced the K^+ uptake by 19.06%, 83.43%, and 75.3%, respectively. These data indicated that both valinomycin (**1**) and streptodepsipeptide P11A (**2**) had the property to significantly induce uptake of K^+ in membrane of erythrocyte.

Some small molecular compounds have been reported to have antitumor activity by targeting tumor metabolic regulators, such as hexokinase (HK) inhibitors: 2-deoxyglucose, lonidamine, and 3-bromopyruvate; PKM2 inhibitor: shikonin and TLN 232; FANS inhibitors: orlista, cerulenin, and EGCG (Galluzzi et al., 2013; Jones and Schulze, 2012; Menendez and Lupu, 2007). It was noted that most of these active antitumor agents targeted only one tumor metabolic regulator. Interestingly, streptodepsipeptide P11A (**2**) had obvious effects on several important tumor metabolic regulators, which were from different metabolic pathways. It has been

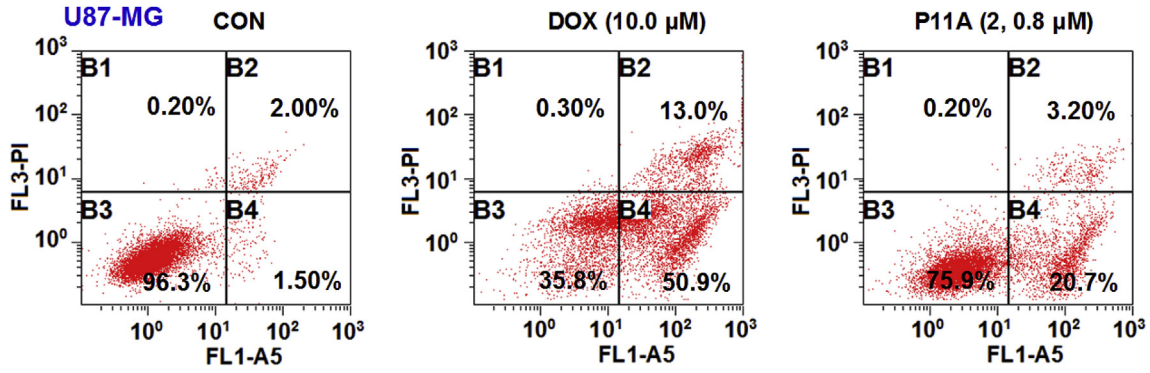

Fig. 5. Streptodepsipeptide P11A (**2**) induced apoptosis in U87-MG cells. U87-MG cells were treated with streptodepsipeptide P11A (**2**) (0.8 μM), DOX (10.0 μM) as positive control, or without compound treatment as negative control (CON) for 72 h, stained with annexin-V FITC and PI, and then analyzed by flow cytometry. (B1: necrotic cells; B2: late apoptotic cells; B3: normal glioma cells; B4: early apoptotic cells).

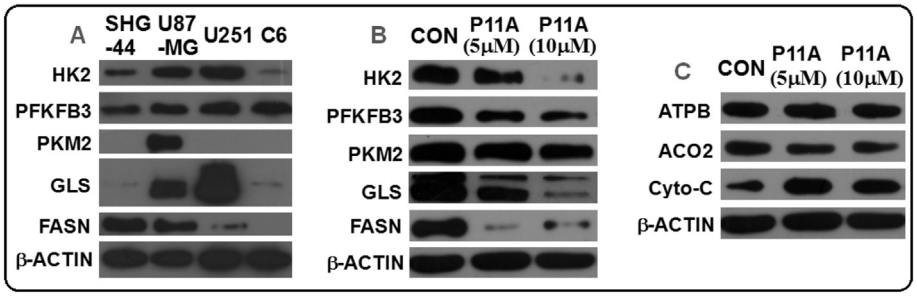

Fig. 6. A: Expression levels of HK2, PFKFB3, PKM2, GLS, and FASN in different glioma cell lines. **B**: Streptodepsipeptide P11A (**2**) reduced expression levels of HK2, PFKFB3, PKM2, GLS, and FASN in U87-MG cells. **C**: Effect of streptodepsipeptide P11A (**2**) on expression levels of ATPB, ACO2, and Cyto-C in U87-MG cells. U87-MG cells were treated with streptodepsipeptide P11A (**2**) (5 and 10 μM) or without streptodepsipeptide P11A (**2**) as negative control (CON) for 48 h. Protein extracted from cells was subjected to western blot analysis (HK2: hexokinase 2; PFKFB3: 6-phosphofructo-2-kinase/2, 6-bisphosphatase 3; PKM2: pyruvate kinase M2; GLS: glutaminase; FASN: fatty acid synthase; β-actin: internal control).

Table 5
Valinomycin (**1**) and streptodepsipeptide P11A (**2**) induced uptake of potassium in membrane of erythrocyte.

Compounds	CON* K+ (mg/mL)	0.01 μM		0.05 μM		0.1 μM	
		K^+ (mg/mL)	+ %*	K^+ (mg/mL)	+ %*	K^+ (mg/mL)	+ %**
1	3.20 ± 0.01	3.81 ± 0.01	19.06	5.87 ± 0.00	83.43	5.62 ± 0.01	75.63
2	3.31 ± 0.01	4.05 ± 0.01	22.36	5.51 ± 0.03	66.46	6.16 ± 0.02	86.10

*CON: Erythrocytes were treated without valinomycin (**1**) and streptodepsipeptide P11A (**2**), +%** = (Compound−CON)/CON × 100%.

proposed that modulating multiple targets could be beneficial for prevention and treatment of complex human diseases such as cancer (Bishayee and Block, 2015; Morphy and Rankovic, 2007). Whether streptodepsipeptide P11A (**2**) has the potential for developing novel anticancer drug need to be further evaluated.

3. Concluding remarks

An actinomycete *Streptomyces* sp. P11-23B that produced antiproliferative cyclodepsipeptides was isolated from a sample of marine mud. Chemical investigation of a crude extract prepared from the cultures of this isolated strain P11-23B resulted in the isolation and identification of two new cyclodepsipeptides, named as streptodepsipeptides P11A (**2**) and P11B (**3**). It was found that both new cyclodepsipeptides significantly suppressed proliferation of four different glioma cell lines. Further investigation demonstrated that streptodepsipeptide P11A (**2**) induced apoptosis in glioma cells, arrested cell cycle at the G_0/G_1 phase, and down-regulated expression levels of HK2, PFKFB3, PKM2, GLS, and FASN, the important tumor metabolic regulators of glycolysis, glutaminolysis, and lipogenesis. These results indicated that regulating multiple glioma metabolic enzymes might be one of the antitumor mechanisms of streptodepsipeptide P11A (**2**). To the best of our knowledge, this is the first report of such a possible mechanism for this class of streptodepsipeptides. However, how streptodepsipeptide P11A (**2**) regulates these metabolic regulators, and what the anti-glioma activity is of this new bioactive cyclodepsipeptide in animal models, need to be further investigated.

4. Experimental section

4.1. General experimental procedures

Melting points were measured with a WRX-4 microscope apparatus and are uncorrected. Optical rotations were measured on a JASCO DIP-370 digital polarimeter. IR spectra were recorded on an AVATAR 370 FT-IR spectrometer (Thermo Nicolet). AA800 atomic absorption spectrometry (PerkinElmer Co., LTD.) was used to determine K+ concentration. NMR spectra were acquired on a Bruker 500 spectrometer using standard pulse programs and acquisition parameters. Chemical shifts were expressed in δ (ppm) and referred to the NMR solvent $CDCl_3$. HRESIMS data were acquired on an Agilent 6230 TOF LC/MS spectrometer. MS-MS data were obtained from AB Triple TOF 5600^{plus} System (AB SCIEX, Framingham, USA) in the optimal MS conditions: scan range *m/z* 100–1500, positive ion mode, source voltage +5.5 kV, source temperature 600 °C, air gas pressure 50 psi, curtain gas (N_2) 30 psi, maximum error ± 5 ppm, collision energy 50 V with a collision energy spread ± 20 V. The separation of pure compounds was conducted on an Agilent 1260 HPLC system with DAD detector. A chirex 3126 (D)-penicillamine column (150 × 4.6 nm, Phenomenex, Shanghai, China) was used for the chiral HPLC analysis. GC analysis was conducted on an Agilent 6890N gas chromatograph system using a DB-624 capillary column (30 m × 0.53 mm, 3.0 μm, Agilent Technologies). N_2 (4.0 mL/min) was used as carrier gas and FID as a detector. The detector and injection port temperatures were set at 250 °C and 200 °C, respectively. The column temperature was 100 °C in 2 min, raised with 10 °C/min to 200 °C, and then kept at 200 °C for 5 min. Octadecyl-functionalized silica gel (ODS, Cosmosil $75C_{18}$ Prep, Nacalai Tesque Inc., Kyoto, Japan) was used for column chromatography (CC). HPLC and analytic grade solvents were purchased from the Sinopharm Chemical Reagent Co. Ltd. (Shanghai, China). Doxorubicin (DOX, >98.0%), D-valine (D-Val), L-valine (L-Val), L-lactate (L-Lac), D-α-hydroxyisovaleric acid (D-Hiv), and D-2-hydroxybutyric acid (D-Hba) were purchased from Sigma. Human glioma U251, U87-MG, and SHG-44 cells, and rat glioma C6 cells were purchased from the Cell Bank of the Chinese Academy of Sciences. Normal human astrocytes (HA, Cat. No. 1800) were obtained from ScienCell. Gause's-agar was purchased from Guangdong Huankai Microbial Science and Technology Co. Ltd. (Guangzhou, China).

4.2. Isolation and identification of marine Streptomyces sp. P11-23B

The strain P11-23B was isolated from a mud sample of marine tidal flat, which was collected from the coast of the East China Sea, close to Zhoushan City, China, in August 2013. The marine mud sample (1.0 g) were dried at 28 °C for 5 days in a sterile culture dish. The dried sample was diluted to 1×10^{-6} g/mL with sterile natural sea water, and then shaken on a rotary shaker at 180 rpm at 28 °C for 10 min. A suspension sample (200 μL) was coated across plates with Gause's-agar medium and then incubated at 28 °C for 7 days. The single colony (strain P11-23B) that grew well was transferred onto Gause's-agar media. Working stocks were prepared on Gause's-agar slants and stored at 4 °C for further use.

The taxonomic identity of isolate strain P11-23B was determined by 16S rDNA sequence analysis, which was conducted by Majorbio (Shanghai, China). The DNA sequence using BLAST (nucleotide sequence comparison) was compared to the GenBank database. The 16S rDNA sequence of strain P11-23B has been deposited in GenBank (accession number: KT933136.1). Voucher strains of *Streptomyces* sp. P11-23B (No. P1123B) are preserved at the Laboratory of Institute of Marine Biology, Ocean College, Zhejiang University, China.

4.3. Fermentation of strain P11-23B

A homogenized colony of isolate P11-23B was transferred into a 500 mL Erlenmeyer flask containing 200 mL of Gause's liquid medium that was incubated for 7 days at 28 °C on a rotary shaker (180 rpm) to produce seed broth. The seed broth (5 mL) was then inoculated into a 500 mL Erlenmeyer flask, which contained 200 mL of Gause's liquid medium. The flasks were incubated at 28 °C on a rotary shaker at 180 rpm for 14 days. A total of 50.0 L fermentation broth was made for this study.

4.4. Isolation of streptodepsipeptides and valinomycin

The fermentation broth of isolated strain P11-23B (50.0 L) was filtered to harvest pellets and fermentation solution. The pellets

were extracted by percolation at room temperature with MeOH three times (2.0 L, 4 h, each) to give a MeOH extract (Part A). The fermentation solution was applied to a column of Diaion HP-20 eluting with H_2O (5.0 L) and then MeOH (5.0 L) to afford MeOH eluent (Part B). Part A and Part B were combined and then concentrated in *vacuo* to yield a crude extract (7.56 g), which was fractionated by ODS CC (800 × 50 mm) eluting in turn with MeOH: H_2O (70:30 and 100:0, v/v) to give two fractions 70M and 100M. Fraction 100M was further fractionated by ODS CC (600 × 30 mm) eluting with MeOH: H_2O (90:10, v/v) to yield 40 fractions (each 20 mL). Fractions 21–30, containing cyclodepsipeptides, were combined and then dried in *vacuo* to furnish crude cyclodepsipeptides. These mixtures were finally separated by HPLC (Zorbax SB-C18 column: 250 × 9.4 mm, 5 μm; mobile phase: MeOH; flow rate: 1.0 mL/min; detection wavelength: 210 nm) to give valinomycin (**1**, 36.8 mg, t_R 20.1 min), streptodepsipeptide P11A (**2**, 17.6 mg, t_R 18.3 min) and streptodepsipeptide P11B (**3**, 6.8 mg, t_R 17.1 min).

*Valinomycin (**1**):* Colorless amorphous powder; molecular formula $C_{54}H_{90}N_6O_{18}$; t_R 20.1 min (MeOH); mp 190–191 °C (lit. 189–190 °C, Pettit et al., 1999); $[\alpha]_D^{25}$ + 18.6° (*c* 0.50, MeOH) (lit. + 16.0°, Pettit et al., 1999); For ^{13}C and ^1H NMR spectroscopic data, see Table S_2; HRESIMS *m/z* $[M+NH_4]^+$ 1128.6647 (calcd for $C_{54}H_{94}N_7O_{18}$, 1128.6655).

*Streptodepsipeptide P11A (**2**):* Colorless amorphous powder; molecular formula $C_{53}H_{88}N_6O_{18}$; t_R 18.3 min (MeOH); $[\alpha]_D^{25}$ + 21.6 (*c* 0.50, MeOH); IR (KBr) ν_{max} 2966, 2874, 2356, 1742, 1655, 1536, 1459, 1196, 1097 cm^{-1}; For ^{13}C and ^1H NMR spectroscopic data, see Table 1; HRESIMS *m/z* $[M-H]^-$ 1095.6051 (calcd for $C_{53}H_{87}N_6O_{18}$, 1095.6077), $[M+H]^+$ 1097.6227 (calcd for $C_{53}H_{89}N_6O_{18}$, 1097.6233).

*Streptodepsipeptide P11B (**3**)*: Colorless amorphous powder; molecular formula $C_{52}H_{86}N_6O_{18}$; t_R 17.1 min (MeOH); $[\alpha]_D^{25}$ + 26.7 (*c* 0.50, MeOH); IR (KBr) ν_{max} 2963, 2871, 2360, 1743, 1655, 1536, 1463, 1193, 1094 m^{-1}; For ^{13}C and ^1H NMR spectroscopic data, see Table 2; HRESIMS *m/z* $[M-H]^-$ 1081.5899 (calcd for $C_{52}H_{85}N_6O_{18}$, 1081.5920).

4.5. Alkaline hydrolysis of streptodepsipeptide P11A (**2**)

Streptodepsipeptide P11A (**2**, 5.0 mg) was hydrolyzed using 3N LiOH (1 mL) in MeOH: H_2O (3:1, v/v) with gentle shaking at room temperature for 12 h. The reaction mixture was neutralized with 3N HCl to pH 6–8 and then dried under reduced pressure to give a residue. Hydrolytic products of **2a** (1.7 mg, t_R 13.1 min), **2b** (1.3 mg, t_R 20.0 min), and **2c** (0.3 mg, t_R 16.1 mi) were next purified from this residue by HPLC using a Zorbax SB-C_{18} column (150 × 4.6 mm, 5 μm) at conditions of flow rate of 1.0 mL/min, detection wavelength of 210 nm, and a gradient mobile phase. MeOH and water were employed as mobile phase A and phase B, respectively. This binary gradient program was 0.0–20.0 min with 10–60% phase A, 20.1–25.0 min with 100% phase A, and 25.1–30.0 with 10% phase A.

*L-Lac-L-Val (**2a**):* Colorless amorphous powder; molecular formula $C_8H_{15}NO_4$; ^1H NMR data (500 MHz, in DMSO-d_6), L-Lac: δ 3.90 (1H, m, H-α), 1.21 (3H, d, J = 6.8 Hz, H_3-β), L-Val: δ 7.48 (1H, d, J = 8.2 Hz, NH-α), 3.90 (1H, m, H-α), 2.05 (1H, m, H-β), 0.81 (3H, d, J = 6.8 Hz, H_3-γ), 0.80 (3H, d, J = 6.8 Hz, H_3-γ); HRESIMS *m/z* $[M+Na]^+$ 212.0890 (calcd for $C_8H_{15}NNaO_4$, 212.0899).

*D-Hiv-D-Val (**2b**)*: Colorless amorphous powder; molecular formula $C_{10}H_{19}NO_4$; ^1H NMR data (500 MHz, in DMSO-d_6), D-Hiv: δ 3.68 (1H, brs, H-α), 1.98 (1H, m, H-β), 0.90 (3H, d, J = 6.8 Hz, H_3-γ), 0.76 (3H, d, J = 6.8 Hz, H_3-γ), D-Val: δ 7.52 (1H, d, J = 8.2 Hz, NH-α), 3.95 (1H, m, H-α), 2.05 (1H, m, H-β), 0.81 (3H, d, J = 6.8 Hz, H_3-γ), 0.80 (3H, d, J = 6.8 Hz, H_3-γ); HRESIMS *m/z* $[M+H]^+$ 218.1402 (calcd for $C_{10}H_{20}NO_4$, 218.1392), $[M+Na]^+$ 240.1204 (calcd for $C_{10}H_{19}NNaO_4$, 240.1212).

*D-Hba-D-Val (**2c**):* Colorless amorphous powder; molecular formula $C_9H_{17}NO_4$; HRESIMS *m/z* $[M-H]^-$ 202.1087 (calcd for $C_9H_{16}NO_4$, 202.1079), $[M+H]^+$ 204.1230 (calcd for $C_9H_{18}NO_4$, 204.1236), $[M+Na]^+$ 226.1053 (calcd for $C_9H_{17}NNaO_4$, 226.1055).

4.6. Acid hydrolysis of valinomycin (**1**), streptodepsipeptides P11A (**2**) and P11B (**3**), L-Lac-L-Val (**2a**), D-Hiv-D-Val (**2b**), and D-Hba-D-Val (**2c**)

Valinomycin (**1**), streptodepsipeptides P11A (**2**), and P11B (**3**) (2.0 mg, each) were individually dissolved in 6N HCl (1.0 mL) and heated at 110 °C in an evacuated glass ampoule for 24 h. After cooling, each hydrolysate was dried under N_2 and then under vacuum to give correspondence residues. Half of each residue was dissolved in H_2O (0.2 mL) to produce sample A for chiral HPLC analysis. The remaining residue was dissolved in MeOH (0.2 mL) to give sample B for GC analysis. In the same way, L-Lac-L-Val (**2a**, 0.5 mg), D-Hiv-D-Val (**2b**, 0.5 mg), and D-Hba-D-Val (**2c**, 0.2 mg) were individually hydrolyzed to give samples C, D, and E, respectively, for chiral HPLC analysis.

4.7. Configuration assignment of each unit in the valinomycin (**1**), streptodepsipeptides P11A (**2**) and P11B (**3**), L-Lac-L-Val (**2a**), D-Hiv-D-Val (**2b**), and D-Hba-D-Val (**2c**)

Each of the samples A, C, D, and E prepared above and the authentic D-Val and L-Val were analyzed using a Chirex 3126 (D)-penicillamine column (150 × 4.6 nm, Phenomenex) with detection at 254 nm and temperature at 22 °C. Aqueous $CuSO_4$ (1 mM) was used as mobile phase. The free amino acids in the acid hydrolysates of valinomycin (**1**), streptodepsipeptides P11A (**2**) and P11B (**3**) were found to be L-valine (t_R, 23.7 min) and D-valine (t_R, 37.1 min) by comparison with retention times of authentic amino acids. The acidic products of L-Lac-L-Val (**2a**), D-Hiv-D-Val (**2b**), and D-Hiv-D-Val (**2c**) were found to be L-Val for 2**a** and D-Val for 2**b** and **2c**. The sample B prepared from each compound was analyzed by GC. GC analyses showed that valinomycin (**1**) and streptodepsipeptide P11B (**3**) produced L-Lac and D-Hiv and streptodepsipeptide P11A (**2**) produced L-Lac, D-Hba, and D-Hiv, as compared with authentic L-Lac (t_R 7.32 min), D-Hba (t_R 8.54 min), and D-Hiv (t_R 9.35 min).

4.8. Biological assays

Sulforhodamine B (SRB) assay. The previously described sulforhodamine B (SRB) assay (Chen et al., 2015; Yu et al., 2014, 2015) was applied to evaluate the activity of the isolated streptodepsipeptides inhibiting the proliferation of glioma U87-MG, U251, SHG-44, and C6 cells. Doxorubicin (DOX) was used as the positive control (CON).

Annexin V-FITC/PI double staining assay. The quantification of apoptotic cells induced by streptodepsipeptide P11A (**2**) was made by annexin V-FITC/PI double staining using an annexin V apoptosis detection kit (Chen et al., 2015; Yu et al., 2014, 2015). Glioma cells were treated with the tested compound for 72 h and flow cytometry was used to determine fluorescence using emission wavelength at 530 nm and 575 nm and excitation wavelength at 488 nm.

Cell cycle assay. Cell cycle perturbation induced by streptodepsipeptide P11A (**2**) was analyzed by propidium iodide (PI) DNA staining using flow cytometry. The detailed protocol is described in Xin et al., 2012.

Western blot analysis. Western blot was used to determine the expression levels of metabolic regulators. The detailed procedure including protein sample preparation, determination of protein concentration, and western blot analysis was carried out as for Yu et al., 2015.

Determination of intracellular K^+ concentration (Bhattacharyya et al., 1971; Li and Yang, 2009; Lu et al., 2006). Briefly, fresh healthy human blood was centrifugated at 660 g for 10 min at 4 °C. The precipitated erythrocytes were washed with GNS (glucose and normal saline injection) buffer (50 g/L glucose and 9 g/L NaCl) and then centrifugated at 660 g for 5 min in three repeated operations. Washed erythrocytes were suspended with GNS buffer (1: 1) to make a 50% erythrocyte suspension. The prepared erythrocyte suspension (1 mL) was treated with different concentrations of tested compounds in the KCl isotonic solution (3 mL) for 90 min at 37 °C. After terminating the treatment by using an ice bath for 1 min, the treated suspension was centrifuged at 660 g for 10 min. The treated erythrocytes were washed with cold GNS (3 mL) five times to remove extracellular K^+, and then haemolyzed by ultrapure H_2O at 4 °C for overnight. Haemolyzed solutions were centrifuged at 10,700 g for 30 min at 4 °C to give cytoplasm and cell membranes. The cell membranes were washed by ultrapure H_2O two times (each 5 mL) to give a wash solution, which was centrifuged at 660 g for 10 min to afford a supernatant. The combination (about 13 mL) of supernatant and cytoplasm was digested by using a mixture (3 mL) of 15.99 mol/L HNO_3 and 11.65 mol/L $HClO_4$ (2:1, v/v) at 140–160 °C for 30 min until a clear and transparent liquid (about 1 mL) appeared. The digested solution was transferred into a volumetric flask (10 mL) and then diluted with 0.1 M HNO_3 to the full volume. The 10 mL digested solution was further diluted with 0.1 M HNO_3 by 50 times to make a final digested solution for the measurement of intracellular K^+ concentration by AA800 atomic absorption spectrometry. A series of accurate K^+ solutions were prepared with KCl to investigate calibration curve ($R^2 = 0.998$). The K^+ concentration of each sample was calculated from the calibration curve.

Conflict of interest

The authors declare no conflict of interest.

Acknowledgments

This study was supported by a grant from the National Natural Science Foundation of China (No. 81273428). We appreciate Mrs. Jianyang Pan (Pharmaceutical Informatics Institute of Zhejiang University) for performing the NMR spectrometry, Dr. Zhiwei Ge and Mrs. Yaer Zhu (the Analysis Center for Agrobiology and Environmental Sciences of Zhejiang University) for MS-MS and GC analyses.

Appendix A. Supplementary data

Supplementary data related to this article can be found at http://dx.doi.org/10.1016/j.phytochem.2016.12.010.

References

Bhattacharyya, P., Epstein, W., Silver, S., 1971. Valinomycin-induced uptake of potassium in membrane vesicles from *Escherichia coli*. Proc. Natl. Acad. Sci. U. S. A. 68, 1488–1492.
Bishayee, A., Block, K., 2015. A broad-spectrum integrative design for cancer prevention and therapy: the challenge ahead. Semin. Cancer Biol. 35, S1–S4.
Chamberlain, M.C., 2010. Temozolomide: therapeutic limitations in the treatment of adult high-grade gliomas. Expert Rev. Neurother. 10, 1537–1544.
Chen, L., Liang, L., Song, T.F., Anjum, K., Wang, W.L., Yu, S.R., Huang, H.C., Lian, X.Y., Zhang, Z.Z., 2015. Synthesis and bioactivity of tripolinolate A from *Tripolium vulgare* and its analogs. Bioorg. Med. Chem. Lett. 25, 2629–2633.
Daye, D., Wellen, K.E., 2012. Metabolic reprogramming in cancer: unraveling the role of glutamine in tumorigenesis. Semin. Cell Dev. Biol. 23, 362–369.
Galluzzi, L., Kepp, O., Vander Heiden, M.G., Kroemer, G., 2013. Metabolic targets for cancer therapy. Nat. Rev. Drug Discov. 12, 829–846.
Guo, D., Bell, E.H., Chakravarti, A., 2013. Lipid metabolism emerges as a promising target for malignant glioma therapy. CNS Oncol. 2, 289–299.
Haynes, D.H., Kowalsky, A., Pressman, B.C., 1969. Application of nuclear magnetic resonance to the conformational changes in valinomycin during complexation. J. Biol. Chem. 244, 502–505.
Heisey, R.M., Huang, J., Mishra, S.K., Keller, J.E., Miller, J.R., Putnam, A.R., D'Silva, T.D.J., 1988. Production of valinomycin, an insecticidal antibiotic, by *Streptomyces griseus var. flexipertum var.* nov. J. Agric. Food Chem. 36, 1283–1286.
Jones, N.P., Schulze, A., 2012. Targeting cancer metabolism-aiming at a tumour's sweet-spot. Drug Discov. Today 17, 232–241.
Kefas, B., Comeau, L., Erdle, N., Montgomery, E., Amos, S., Purow, B., 2010. Pyruvate kinase M2 is a target of the tumor-suppressive microRNA-326 and regulates the survival of glioma cells. Neurol. Oncol. 12, 1102–1112.
Kessler, R., Bleichert, F., Eschrich, K., 2008. 6-Phosphofructo-2-kinase/fructose-2,6-bisphosphatase (PFKFB3) is up-regulated in high-grade astrocytomas. J. Neurooncol. 86, 257–264.
Li, Y.H., Yang, W.B., 2009. Selenium determination in the tea by atomic fluorescence spectrometry method after digesting by nitric acid combining perchloric acid. Environ. Sci. Surv. 28, 80–81.
Liang, Y., Xie, X., Chen, L., Yan, S.L., Ye, X.W., Anjum, K., Huang, H.C., Lian, X.Y., Zhang, Z.Z., 2016. Bioactive polycyclic quinones from marine *Streptomyces* sp. 182SMLY. Mar. Drugs 14, 10.
Lim, T.H., Oh, H., Kwon, S.Y., Kim, J.H., Seo, H.W., Lee, J.H., Min, B.S., Kim, J.C., Lim, C.H., Cha, B., 2007. Antifungal activity of valinomycin, a cyclodepsipeptide from *Streptomyces padanus* TH-04. Nat. Prod. Sci. 13, 144–147.
Lu, J., Jiang, Y.C., Hu, M.C., Li, S.N., Wang, Y.S., 2006. Rb^+ uptake by human erythrocytes and its transmembrane pathway. Chin. J. Chem. 24, 350–354.
Lu, W., Pelicano, H., Huang, P., 2010. Cancer metabolism: is glutamine sweeter than glucose? Cancer Cell 18, 199–200.
Menendez, J.A., Lupu, R., 2007. Fatty acid synthase and the lipogenic phenotype in cancer pathogenesis. Nat. Rev. Cancer 7, 763–777.
Mittal, S., Pradhan, S., Srivastava, T., 2015. Recent advances in targeted therapy for glioblastoma. Expert Rev. Neurother. 15, 935–946.
Morphy, R., Rankovic, Z., 2007. Fragments, network biology and designing multiple ligands. Drug Discov. Today 12, 156–160.
Newman, D.J., Cragg, G.M., 2014. Marine-sourced anti-cancer and cancer pain control agents in clinical and late preclinical development. Mar. Drugs 12, 255–278.
Park, C.N., Lee, J.M., Lee, D., Kim, B.S., 2008. Antifungal activity of valinomycin, a peptide antibiotic produced by *Streptomyces* sp. strain M10 antagonistic to *Botrytis cinerea*. J. Microb. Biotech. 18, 880–884.
Patil, S.A., Hosni-Ahmed, A., Jones, T.S., Patil, R., Pfeffer, L.M., Miller, D.D., 2013. Novel approaches to glioma drug design and drug screening. Expert Opin. Drug Discov. 8, 1135–1151.
Petit, K., Biard, J.F., 2013. Marine natural products and related compounds as anticancer agents: an overview of their clinical status. Anticancer Agents Med. Chem. 13, 603–631.
Pettit, G.R., Tan, R., Melody, N., Kielty, J.M., Pettit, R.K., Herald, D.L., Tucker, B.E., Mallavia, L.P., Doubeka, D.L., Schmidt, J.M., 1999. Antineoplastic agents. Part 409: isolation and structure of montanastatin from a terrestrial actinomycete. Bioorg. Med. Chem. 7, 895–899.
Ru, P., Williams, T.M., Chakravarti, A., Guo, D., 2013. Tumor metabolism of malignant gliomas. Cancers 5, 1469–1484.
Santos, C.R., Schulze, A., 2012. Lipid metabolism in cancer. FEBS J. 279, 2610–2623.
Schumacher, M., Kelkel, M., Dicato, M., Diederich, M., 2011. Gold from the sea: marine compounds as inhibitors of the hallmarks of cancer. Biotechnol. Adv. 29, 531–547.
Tabeta, R., Saito, H., 1985. High-resolution solid-state ^{13}C NMR study of free and metal-complexed macrocyclic antibiotic ionophores valinomycin, nonactin, and tetranactin: conformational elucidation in solid and solution by conformation-dependent ^{13}C chemical shifts. Biochemistry 24, 7696–7702.
Vander Heiden, M.G., 2011. Targeting cancer metabolism: a therapeutic window opens. Nat. Rev. Drug Discov. 10, 671–684.
Wolf, A., Agnihotri, S., Micallef, J., Mukherjee, J., Sabha, N., Cairns, R., Hawkins, C., Guha, A., 2011. Hexokinase 2 is a key mediator of aerobic glycolysis and promotes tumor growth in human glioblastoma multiforme. J. Exp. Med. 208, 313–326.
Wu, C.Y., Jan, J.T., Ma, S.H., Kuo, C.J., Juan, H.F., Cheng, Y.S., Hsu, H.H., Huang, H.C., Wu, D., Brik, A., Liang, F.S., Liu, R.S., Fang, J.M., Chen, S.T., Liang, P.H., Wong, C.H., 2004. Small molecules targeting severe acute respiratory syndrome human coronavirus. Proc. Natl. Acad. Sci. U. S. A. 101, 10012–10017.
Xin, W.X., Ye, X.W., Yu, S.R., Lian, X.Y., Zhang, Z.Z., 2012. New capoamycin-type antibiotics and polyene acids from marine *Streptomyces fradiae* PTZ0025. Mar. Drugs 10, 2388–2402.
Yu, S.R., Ye, X.W., Chen, L., Lian, X.Y., Zhang, Z.Z., 2014. Polyoxygenated 24,28-epoxyergosterols inhibiting the proliferation of glioma cells from sea anemone *Anthopleura midori*. Steroids 88, 19–25.
Yu, S.R., Ye, X.W., Huang, H.C., Peng, R., Su, Z.H., Lian, X.Y., Zhang, Z.Z., 2015. Bioactive sulfated saponins from sea cucumber *Holothuria moebi*i. Planta Med. 81, 152–159.